ELSEVIER

Journal of Organometallic Chemistry 483 (1994) 7–15

Journal of Organometallic Chemistry

# Synthesis, X-ray crystal structure, and redox properties of Cp*Ru(NO)(mnt)

Kaiyuan Yang, Simon G. Bott *, Michael G. Richmond *

*Center for Organometallic Research and Education, Department of Chemistry, University of North Texas, Denton, TX 76203, USA*

Received 26 October 1993; in revised form 14 March 1994

**Abstract**

The cyclopentadienylruthenium complex $Cp^*Ru(NO)Cl_2$ reacts with disodium maleonitriledithiolate ($Na_2mnt$) in methanol to give Cp*Ru(NO)(mnt) in 85% yield. The product has been characterized in solution by IR and NMR ($^1H$ and $^{13}C$) spectroscopies. Cp*Ru(NO)(mnt) crystallizes in the orthorhombic space group *Pbca* with $a = 7.6042(7)$, $b = 16.368(2)$, $c = 26.138(3)$ Å, $V = 3253.2(6)$ Å$^3$, and $Z = 8$. Full-matrix least-squares refinement yielded $R = 0.043$ for 777 ($F > 6\sigma(F)$) reflections. The electrochemical properties of Cp*Ru(NO)(mnt) have been investigated by cyclic and rotating disk electrode voltammetric, and bulk electrolytic methods. Two redox responses were observed and assigned to $0/+1$ and $0/-1$ couples. The composition of the HOMO and LUMO levels in Cp*Ru(NO)(mnt) has been examined by extended Hückel molecular orbital calculations, and the results discussed with respect to the electrochemical data.

*Keywords:* Ruthenium; Nitrosyls; Maleonitriledithiolate; Electrochemistry; Extended Hückel calculations

## 1. Introduction

The synthesis and study of organometallic complexes possessing an ancillary maleonitriledithiolate (mnt) ligand(s) have continued to receive attention [1–15]. Such complexes have been thoroughly investigated in electron-transfer reactions and for their luminescent behavior by Eisenberg [16–21] and Volger [22]. Moreover, reports of spin exchange between the conduction electrons of certain mnt-substituted complexes suggest that these complexes may function as models for low-dimensional molecular metals [23,24]. While the vast majority of mnt-substituted complexes are based on the metals of platinum, cobalt, nickel, and iron, few ruthenium-substituted mnt complexes exist. Recently, Stiefel and coworkers have reported the synthesis and redox properties of $Ru(bpy)_2(mnt)$ [25].

Here we report our results on the synthesis, X-ray diffraction structure, and electrochemical properties of Cp*Ru(NO)(mnt). Extended Hückel molecular orbital calculations have been carried out, and the theoretical data discussed with respect to the electrochemical data.

## 2. Results and discussion

### 2.1. Synthesis and spectral characterization of Cp*Ru(NO)(mnt)

Treatment of a methanol solution of $Cp^*Ru(NO)Cl_2$ (**1**) with a slight excess of disodium maleonitriledithiolate ($Na_2mnt$) [26] led to an immediate color change from green to red–brown. After stirring overnight at room temperature, the methanol was removed and the solid taken up in $CH_2Cl_2$, followed by chromatography over silica gel. Cp*Ru(NO)(mnt) (**2**) was subsequently isolated in 85% yield as an air stable, black solid (Eq. (1)).

Complex **2** is very soluble in polar solvents but only slightly soluble in non-polar solvents. The IR spectrum of **2** in $CH_2Cl_2$ displays an intense $\nu$NO band at 1767 $cm^{-1}$, which is readily attributed to the linear nitrosyl group [27]. The coordinated mnt ligand exhibits two medium intensity $\nu$CN stretches at 2213 and 2206

* Corresponding authors.


*SSDI* 0022-328X(94)24686-D

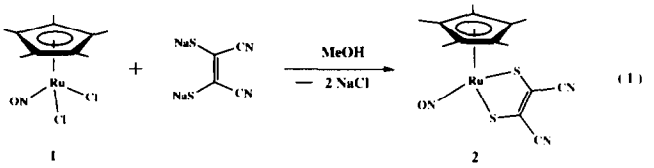


(1)

1 2

$cm^{-1}$, assigned to the vibrationally coupled asymmetric and symmetric C≡N stretches, respectively, along with a weak mnt-alkene $\nu$(C=C) stretch at 1606 $cm^{-1}$ [28,29]. A single resonance at $\delta = 1.86$ is observed in the $^1$H-NMR spectrum of Cp*Ru(NO)(mnt) and is assigned to the methyl protons of the Cp* ring while the $^{13}$C-NMR spectrum of **2** exhibits resonances at $\delta = 9.6$, 111.5, 115.7, and 125.8. The former two resonances belong to the cyclopentadienyl methyl and ring carbons, respectively, with the latter two resonances being assigned to the nitrile and alkene carbons, respectively, based on the reported chemical shifts of related compounds [30].

### 2.2. Solid-state structure of Cp*Ru(NO)(mnt)

Single crystals of **2** suitable for X-ray diffraction analysis were grown from a dichloromethane solution of **2** that had been layered with heptane. Cp*Ru(NO)(mnt) exists as discrete molecules in the unit cell with no unusually short inter- or intramolecular contacts. The X-ray data collection and processing parameters for **2** are given in Table 1 with the fractional coordinates listed in Table 2.

Table 1
X-Ray crystallographic and data processing parameters for Cp*Ru(NO)(mnt) (**2**)

| | |
|---|---|
| Space group | *Pbca* |
| Cell Constants | |
| $a$ (Å) | 7.6042(7) |
| $b$ (Å) | 16.368(2) |
| $c$ (Å) | 26.138(3) |
| $V$ (Å$^3$) | 3253.2(6) |
| Molecular formula | $C_{14}H_{15}N_3ORuS_2$ |
| FW | 406.49 |
| Formula units/cell ($Z$) | 8 |
| $\rho$ (g $cm^{-3}$) | 1.660 |
| Crystal size ($mm^3$) | 0.18×0.15×0.44 |
| Absorption coefficient ($\mu$) ($cm^{-1}$) | 11.93 |
| $\lambda$ (radiation) (Å) | 0.71073 |
| Data collection method | $\omega$ |
| Collection range (°) | $2.0 \le 2\theta \le 40.0$ |
| Total no. of data collected | 1796 |
| No. of independent observed data | 777 |
| $R$ | 0.043 |
| $R_w$ | 0.049 |
| Weights | $w = [0.04F^2 + (\sigma F)^2]^{-1}$ |

Table 2
Positional parameters of the non-hydrogen atoms for Cp*Ru(NO)(mnt) (**2**) with estimated standard deviations in parentheses

| Atom | $x$ | $y$ | $z$ | $U$ [a] |
|---|---|---|---|---|
| Ru | 0.0329(2) | 0.18942(8) | 0.10382(5) | 2.07(2) |
| S1 | 0.0504(6) | 0.3290(2) | 0.0839(2) | 3.0(1) |
| S2 | −0.1518(6) | 0.2277(3) | 0.1709(2) | 2.76(9) |
| O | −0.177(2) | 0.1131(8) | 0.0266(5) | 5.8(4) |
| N | −0.117(2) | 0.1546(8) | 0.0586(5) | 3.2(3) |
| N3 | −0.096(2) | 0.5345(9) | 0.1261(8) | 7.0(6) |
| N4 | −0.344(2) | 0.4042(8) | 0.2367(6) | 4.1(4) |
| C1 | −0.077(2) | 0.3747(9) | 0.1314(6) | 2.9(4) [b] |
| C2 | −0.162(2) | 0.3340(8) | 0.1665(6) | 2.2(3) [b] |
| C3 | −0.086(2) | 0.463(1) | 0.1301(6) | 3.4(4) [b] |
| C4 | −0.268(2) | 0.3736(9) | 0.2056(6) | 2.9(4) [b] |
| C11 | 0.281(2) | 0.186(1) | 0.1462(5) | 2.1(3) [b] |
| C12 | 0.188(2) | 0.113(1) | 0.1608(7) | 3.5(4) [b] |
| C13 | 0.160(2) | 0.0681(9) | 0.1144(6) | 2.6(3) [b] |
| C14 | 0.253(2) | 0.1087(9) | 0.0749(6) | 2.4(3) [b] |
| C15 | 0.327(2) | 0.1784(9) | 0.0933(5) | 2.3(3) [b] |
| C111 | 0.335(2) | 0.246(1) | 0.1837(7) | 3.9(4) [b] |
| C121 | 0.127(3) | 0.087(1) | 0.2127(7) | 4.1(4) [b] |
| C131 | 0.074(3) | −0.014(1) | 0.1130(7) | 4.8(5) [b] |
| C141 | 0.267(3) | 0.076(1) | 0.0220(7) | 5.1(5) [b] |
| C151 | 0.450(3) | 0.235(1) | 0.0676(7) | 4.5(4) [b] |

[a] Anisotropically refined atoms are given in the form of the isotropic equivalent displacement parameter defined as: $(4/3)*[a^2*B_{1,1} + b^2B_{2,2} + c^2B_{3,3} + ab(\cos\gamma)*B_{1,2} + ac(\cos\beta)*B_{1,3} + bc(\cos\alpha)*B_{2,3}$.
[b] Atoms were refined isotropically.

The ORTEP diagram in Fig. 1 shows the molecular structure of **2** and confirms the six-coordinate geometry about the ruthenium atom, assuming the Cp* ring serves as a three-coordinate ligand. The molecule possesses idealized $C_s$ molecular symmetry as is commonly observed with many three-legged piano-stool complexes. Selected bond distances and angles are given in Table 3. The two Ru–S distances of 2.347(4) and 2.332(5) Å are in agreement with the distances reported for other metal–sulfur complexes [6,7,21,31], while the Ru–$N_{(nitrosyl)}$ length of 1.74(1) Å [32,33] and

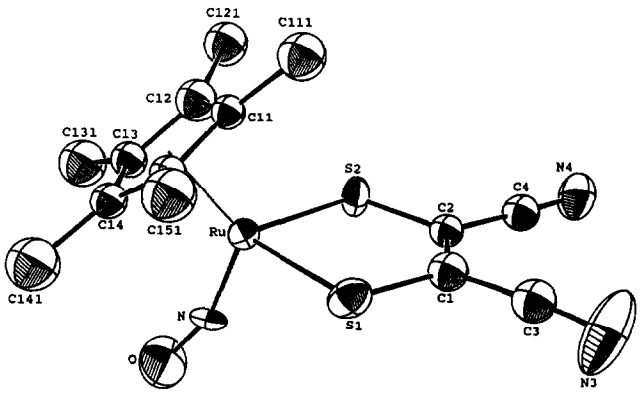


Fig. 1. ORTEP diagram of Cp*Ru(NO)(mnt) with the thermal ellipsoids drawn at the 50% probability level.

Table 3
Selected bond lengths (Å) and angles (°) in Cp*Ru(NO)(mnt) (2) [a]

| | | | |
|---|---|---|---|
| *Bond distances* | | | |
| Ru–S(1) | 2.347(4) | Ru–S(2) | 2.332(5) |
| Ru–N | 1.74(1) | Ru–C(11) | 2.19(1) |
| Ru–C(12) | 2.27(2) | Ru–C(13) | 2.22(1) |
| Ru–C(14) | 2.26(2) | Ru–C(15) | 2.26(1) |
| S(1)–C(1) | 1.74(2) | S(2)–C(2) | 1.75(1) |
| O–N | 1.17(2) | N(3)–C(3) | 1.18(2) |
| N(4)–C(4) | 1.12(2) | C(1)–C(2) | 1.31(2) |
| C(1)–C(3) | 1.45(2) | C(2)–C(4) | 1.45(2) |
| *Bond angles* | | | |
| S(1)–Ru–S(2) | 86.5(2) | S(1)–Ru–N | 101.8(4) |
| S(1)–Ru–C(11) | 95.0(4) | S(1)–Ru–C(12) | 130.5(4) |
| S(1)–Ru–C(13) | 150.7(4) | S(1)–Ru–C(14) | 116.9(4) |
| S(1)–Ru–C(15) | 89.7(4) | S(2)–Ru–N | 101.8(5) |
| N–Ru–C(11) | 154.3(6) | N–Ru–C(12) | 127.4(6) |
| N–Ru–C(13) | 94.4(6) | N–Ru–C(14) | 93.9(6) |
| N–Ru–C(15) | 122.7(6) | Ru–S(1)–C(1) | 103.2(5) |
| Ru–S(2)–C(2) | 104.3(5) | Ru–N–O | 159.(1) |
| S(1)–C(1)–C(2) | 124.(1) | S(1)–C(1)–C(3) | 116.(1) |
| C(2)–C(1)–C(3) | 120.(1) | S(2)–C(2)–C(1) | 122.(1) |
| S(2)–C(2)–C(4) | 115.(1) | C(1)–C(2)–C(4) | 123.(1) |
| N(3)–C(3)–C(1) | 176.(2) | N(4)–C(4)–C(2) | 177.(2) |

[a] Numbers in parentheses are estimated standard deviations in the least significant digits.

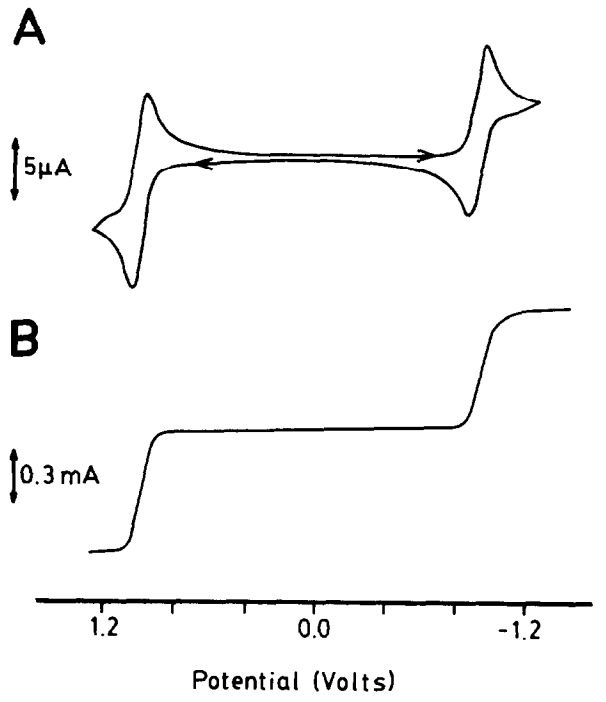


Fig. 2. (A) cathodic scan cyclic voltammogram of ca. $1\times10^{-3}$ M Cp*Ru(NO)(mnt) at room temperature in MeCN containing 0.25 M TBAP at 0.1 V $s^{-1}$, and (B) rotating disk electrode voltammogram of ca. $2.5\times10^{-3}$ M Cp*Ru(NO)(mnt) in MeCN containing 0.25 M TBAP at 0.05 V $s^{-1}$.

the 159(1)° bond angle observed for the Ru–N–O linkage [34] are unexceptional with regard to other linear nitrosyl complexes. The bond lengths and angles of the coordinated-mnt and the cyclopentadienyl ligands in (2) are unexceptional and require no comment.

### 2.3. Electrochemical studies

Cyclic voltammetry studies on Cp*Ru(NO)(mnt) were carried out at a platinum electrode in either $CH_2Cl_2$, THF, or MeCN solvent containing 0.25M tetra-*n*-butylammonium perchlorate (TBAP) as the supporting electrolyte. No major differences were observed in the cyclic voltammograms (CV) as a function of the solvent at room temperature. Fig. 2(A) shows the CV of Cp*Ru(NO)(mnt) in MeCN solvent at room temperature. Two well-defined, reversible redox couples at $E_{1/2} = 1.04$ and $-0.92$ V are observed at a scan rate of 100 mV $s^{-1}$, which have been assigned to the $0/+1$ and $0/-1$ redox couples, respectively, as outlined in Eq. (2). Both redox couples exhibit current ratios ($i_p^a/i_p^c$) of near unity, and plots of the current function ($i_p$) vs. the square root of the scan rate ($v$) are linear over the scan rates examined. Calibration of the

Table 4
Cyclic voltammetric data for Cp*Ru(NO)(mnt) [a]

| Redox Couple: [b] | $0/+1$ | | | | $0/-1$ | | | |
|---|---|---|---|---|---|---|---|---|
| Solvent/Temp [c] | $E_p^a$ | $E_p^c$ | $i_p^c/i_p^a$ | $E_{1/2}$ | $E_p^c$ | $E_p^a$ | $i_p^a/i_p^c$ | $E_{1/2}$ |
| MeCN/RT | 1.08 | 1.00 | 0.90 | 1.04 | −0.97 | −0.88 | 0.89 | −0.92 |
| MeCN/−30°C | 1.07 | 1.01 | 1.0 | 1.04 | −0.96 | −0.88 | 1.0 | −0.92 |
| THF/RT | 1.12 | 1.01 | 0.71 | 1.07 | −1.03 | −0.92 | 0.61 | −0.98 |
| THF/0°C | 1.03 | 1.14 | 0.80 | 1.09 | −1.05 | −0.83 | [d] | [d] |
| THF/−30°C | 1.05 | 1.17 | 0.80 | 1.11 | −1.04 | −0.66 | [d] | [d] |
| THF/−67°C | 0.99 | 1.12 | 0.89 | 1.06 | −0.99 | −0.76 | [d] | [d] |
| $CH_2Cl_2$/RT | 1.10 | 1.02 | 1.0 | 1.06 | −1.07 | −0.98 | 0.82 | −0.98 |
| $CH_2Cl_2$/−67°C | 1.10 | 1.04 | 1.1 | 1.07 | −1.19 | −0.90 | [d] | [d] |

[a] All cyclic voltammograms were recorded in solutions containing 0.25 M TBAP at a scan rate of 0.1 V $s^{-1}$. Potentials are in volts relative to a silver wire quasi-reference electrode, calibrated against added ferrocene. [b] $E_p^a$ and $E_p^c$ refer to the anodic and cathodic peak potentials for a given redox couple. The half-wave potential $E_{1/2}$, which represents the chemically reversible redox couple, is defined as $(E_p^a + E_p^c)/2$. [c] All temperatures have been measured with the aid of a digital thermometer and are considered to be accurate to within ±1°C. [d] No reverse redox couple was observed.

peak currents ($i_p$) against ferrocene, coupled with the data obtained from rotating disk electrode (RDE) voltammetry experiments, unequivocally establishes the reversible, one-electron nature of the oxidation and reduction waves under the given conditions [35]. When the same CV sample was examined at −30°C, both redox couples exhibited increased stability, as judged by the calculated current ratio of unity for each redox couple. Table 4 shows these data along with the CV data as a function of the solvent and temperature.

Cp*Ru(NO)(mnt) was also examined at a platinum electrode by rotating disk voltammetry in MeCN solvent at room temperature containing 0.25 M TBAP. The RDE voltammogram shown in Fig. 2(B) reveals the presence of a well-defined oxidation and reduction wave. The half-wave potential for the 0/+1 redox couple is observed at 1.00 V while the half-wave potential for the 0/−1 redox couple is found at −0.99 V. These $E_{1/2}$ values from the RDE voltammogram are essentially the same as those obtained from the CV of Cp*Ru(NO)(mnt). The Nernstian nature of both couples was readily demonstrated by plots of $E$ vs. $\log[(i_d - i)/i]$, which afforded slopes close to the theoretically predicted value of 59.1 mV for a reversible, one-electron transfer process [35]. A value of 64 mV and 70 mV for the 0/+1 and 0/−1, respectively, was obtained when the RDE data were analyzed according to the relationship developed by Tomeš (i.e. $|E_{3/4}-E_{1/4}|$) [36], consistent with the proposed one-electron nature of these couples. No kinetic complications were observed with these couples based on the linearity observed in the plots of $i_d$ vs. $\omega^{1/2}$ over the electrode rotation rate of 200–1200 rev $min^{-1}$ [37]. When these data were examined with the Levich equation, a diffusion coefficient ($D_0$) of $1.17 \times 10^{-5}$ and $1.07 \times 10^{-5}$ $cm^2$ $s^{-1}$ for the oxidation and the reduction wave respectively, was calculated for Cp*Ru(NO)(mnt). The experimentally measured values of $D_0$ are in excellent agreement with the theoretically calculated value for $D_0$ of $1.00 \times 10^{-5}$ $cm^2$ $s^{-1}$, determined by using the crystallographic data and the Stokes-Einstein equation (Eq. (3)) [38]:

$$D_0 = (1 \times 10^7) RT/6\pi rN\eta \quad (3)$$

While the effect of the solvent on the CV of **2** at room temperature is very similar, both THF and $CH_2Cl_2$ were found to yield a reduction couple that is extremely temperature dependent. These data are summarized in Table 4, with the CV's of Cp*Ru(NO)(mnt) in THF solvent as a function of temperature being shown in Fig. 3. The cyclic voltammograms in $CH_2Cl_2$ mirror those recorded in THF and are not shown. Fig. 3(A) shows the room temperature CV of Cp*Ru(NO)(mnt) and the presence of two major redox couples, whose assignments are identical to those in MeCN solvent. However, unlike the CV recorded in MeCN, the 0/+1 and 0/−1 redox couples are not as stable as those in MeCN based on the diminished current ratio of 0.71 and 0.61, respectively, and the presence of redox responses at 0.00 and −0.15 V. These latter CV waves were shown to originate from the 0/−1 redox couple. Lowering the temperature to 0°C reveals the existence of a significant change in the 0/−1 redox couple, as shown in Fig. 3(B), where a potential shift of 90 mV is observed in the anodic direction of the reverse wave. At this temperature the 0/+1 redox couple experiences a slight stabilization as evidenced by the increased current ratio of 0.80. Further cooling to −30°C and −67°C affords the CV's shown in Fig. 3(C) and 3(D) respectively; the CV behavior at these temperatures mirrors that observed in Fig. 3(B) which was obtained at 0°C.

This separation of the anodic couple from the 0/−1 redox wave as the temperature is lowered signals the irreversible nature of the initial reduction product $\mathbf{2}^{-\cdot}$. One such scenario for this behavior involves the bending of the nitrosyl ligand, as illustrated in Eq. (4). Here the rate constant ($k_{-1}$) for the bent-to-linear nitrosyl transformation is slow at low temperatures in $CH_2Cl_2$ and THF solvents, making the reduction process irreversible. Repetitive scanning from 0 to −1.3 V in the low-temperature CV's did not yield any evidence for the reversibility of the anodic wave derived from the 0/−1 redox couple. The overall process outlined in Eq. (4) conforms to an ECE scheme [35] and has been invoked in the reduction of $CpM(CO)_2(NO)$ (where M = Cr, Mo) [39,40].

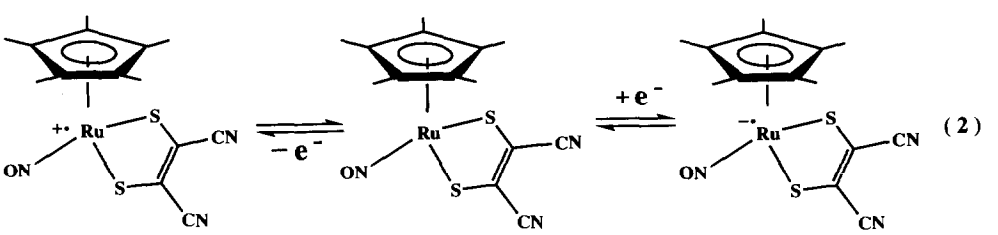

Cp*Ru(NO)(mnt) was next examined by constant-potential coulometry in order to verify the electron stoichiometry associated with each individual redox process and to explore the effect of oxidation/reduction on the IR stretching bands of the nitrosyl and mnt ligands. Cp*Ru(NO)(mnt) was oxidized electrochemically at 1.20 V in $CH_2Cl_2$ solvent containing 0.25 M TBAP at −78°C. This solvent was chosen because of the unity value found for the current ratio ($I_p^c/I_p^a$) and the absence of solvent overlap with the nitrile bands in the IR spectrum. The total charge passed upon completion of the oxidation was $Q = 0.97$ coulombs per mole of **2** in agreement with the one-electron nature of this redox couple. IR analysis of the anolyte at −70°C revealed the presence of two new bands at 2338 (m) and 1833 (vs) $cm^{-1}$. The higher frequency band is assigned to the C≡N stretch of the mnt ligand while the other IR band belongs to the linear nitrosyl group. The observed high-frequency shifts of these ligands are consistent with an oxidation process that takes place at a metal-based HOMO, which is accompanied by a concomitant decrease in the ability of the ruthenium center to back donate electron density into the $\pi^*$ orbitals of the nitrosyl and mnt ligands [41,42]. Attempts to isolate $2^{+\cdot}$ were unsuccessful as only neutral **2** was obtained. The thermally sensitive nature of $2^{+\cdot}$ was demonstrated by allowing a solution of electrochemically generated $2^{+\cdot}$ to warm up from −78°C to room temperature. Here decomposition is noticeable starting at −40°C, being complete by room temperature. The IR spectrum of this solution at room temperature revealed the presence of **2** along with new IR bands at 1820 and 1608 $cm^{-1}$. **2** could be isolated in 60% yield by column chromatography, but the unknown material was irreversibly adsorbed onto the silica gel and no further effort was directed at its isolation.

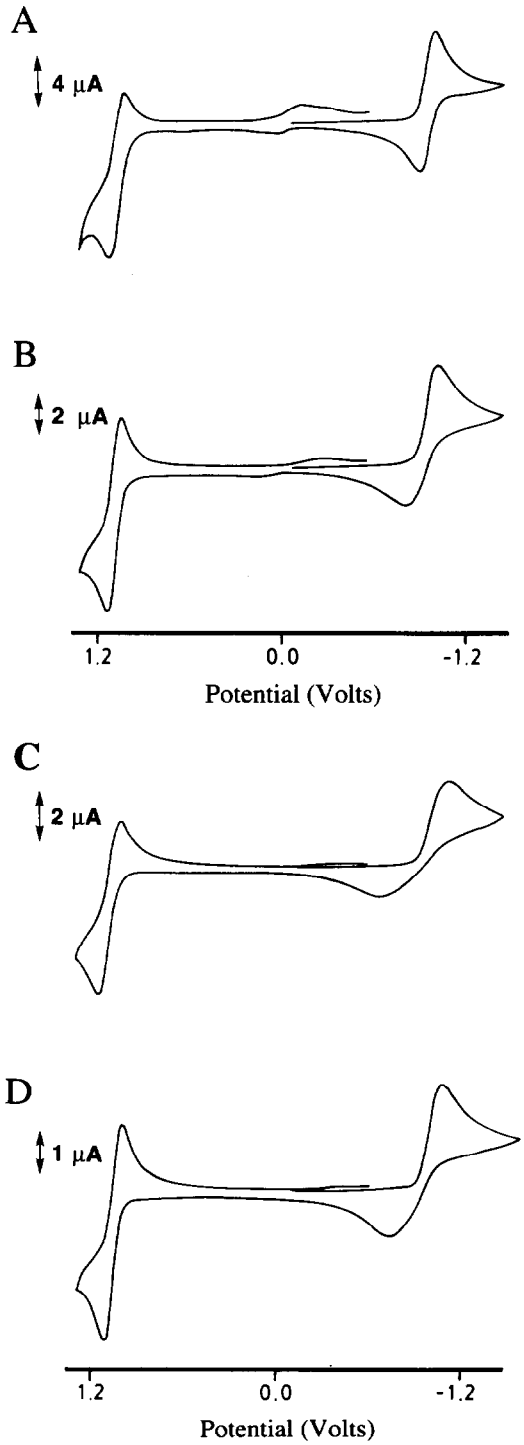


Fig. 3. Cathodic scan cyclic voltammograms of ca. $1 \times 10^{-3}$ M Cp*Ru(NO)(mnt) in THF containing 0.25 M TBAP at 0.1 V $s^{-1}$ as a function of temperature: (A) room temperature, (B) 0°C, (C) −30°C, and (D) −67°C.

The controlled-potential electrolysis of Cp*Ru(NO)(mnt) at −1.2 V was also explored in $CH_2Cl_2$ and MeCN solvent containing 0.25 M TBAP. Unlike the one-electron oxidation process observed during bulk electrolysis, the total charge passed during our reductions ranged from $Q = 1.5$ to 1.9 coulombs per mole of **2** in $CH_2Cl_2$ at −78°C and from $Q = \sim 4.0$ to 5.0 coulombs per mole of **2** at room temperature for both solvents. The consumption of more than two electrons is inconsistent with the one-electron nature of the 0/−1 redox couple determined by the CV and RDE experiments. IR analysis of this extremely oxygen-sensitive catholyte solution showed only the presence of a single $\nu$(CN) band at 2185 $cm^{-1}$. No terminal nitrosyl band was noticed over the spectral range of 2000–1600 $cm^{-1}$. Unfortunately, we were not able to explore the region below 1600 $cm^{-1}$ owing to IR contributions from the solvent and the electrolyte.

The CV of the unknown material after electrolysis (not shown) revealed a prominent irreversible oxidation wave at $E_p^a = -0.2$ V at a scan rate of 0.1 V $s^{-1}$. The observed $E_p^a$ values were found to be dependent on the scan rate ($v$) as expected for an irreversible,

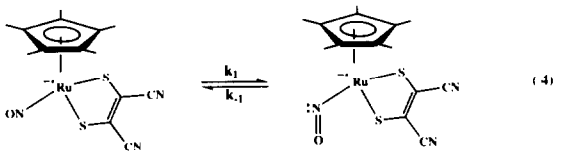


one-electron transfer. A plot of $E_p^a$ vs. log ($\upsilon$) afforded a slope on the order of 96 mV per decade, which is greater than the theoretically predicted 30 mV per decade slope for a reversible electron-transfer step [43].

### 2.4. Extended Hückel calculations

The nature of the HOMO and LUMO in Cp*Ru(NO)(mnt) was examined by extended Hückel molecular orbital calculations. Fig. 4 shows the three-dimensional CACAO drawings of the molecular orbitals [44]. The HOMO in Cp*Ru(NO)(mnt) occurs at $\sim -11.3$ eV and is primarily a ruthenium-based orbital ($dx^2 - y^2$ with a small amount of $dz^2$ hybridization); minor out-of-phase contributions from the non-bonding electron pairs from the sulfur atoms and the nitrosyl ligand along with in-phase Cp*–Ru overlap are also readily observed. An analogous out-of-phase interaction between the p-type lone electron pair on the thiolate ligand and a filled d-orbital has been reported in $CpMo(NO)(SH)_2$ by Enemark [45]. We have seen this same HOMO pattern in other mnt-substituted complexes that are derived from the mnt ligand and $d^8$-$ML_4$ fragments of the form CpML [46]. It is of interest to emphasize that the formal oxidation of the ruthenium center certainly accounts for the observed high frequency IR shifts in the nitrosyl and nitrile stretching bands in $[Cp^*Ru(NO)(mnt)]^{+\cdot}$ (vide supra).

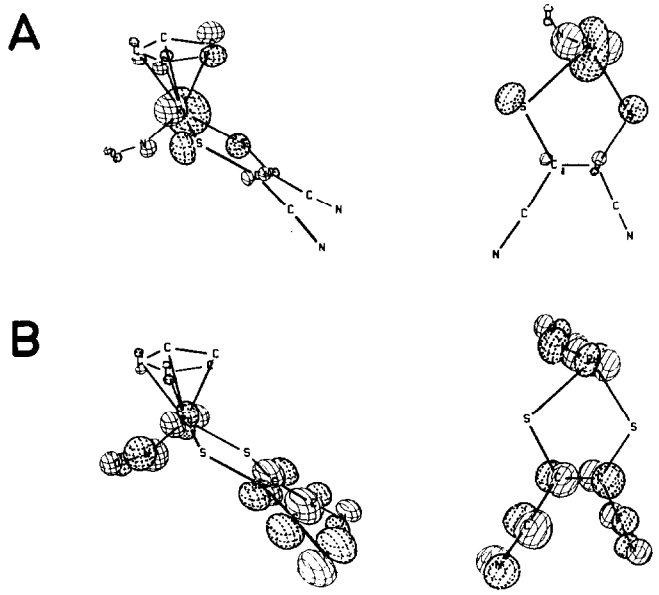


Fig. 4. CACAO drawings of the HOMO (A) and LUMO (B) of Cp*Ru(NO)(mnt). The Cp*-methyl groups have been eliminated from the side-view drawings on the left while the Cp* ring has been eliminated from the top-view drawing on the right.

The LUMO in Cp*Ru(NO)(mnt) ($\sim -9.5$ eV) is composed of major contributions from the ruthenium, the nitrosyl group, and the mnt ligand. The $d\pi$–$p\pi$ overlap between the ruthenium $dxz$ orbital (hybridized with some $dxy$) and the nitrosyl ligand is antibonding, with an added contribution from the ancillary $\pi^*$ mnt ligand. The nodal pattern of the mnt ligand in Cp*Ru(NO)(mnt) is similar to $\Psi_4$ of the isolated six $\pi$-electron dithiol compound *cis*-(HS)(CN)C=C(CN)(SH). It is not immediately clear as to the initial site of electron accession in the $0/-1$ redox couple, but we favor electron association with the RuNO linkage in Cp*Ru(NO)(mnt) given the loss of the IR band of the terminal nitrosyl group after bulk electrolysis and the published ESR data that support nitrosyl bending in CpM(CO)(NO) (where M = Cr, Mo) during electrochemical reduction [39,47]. Future MO calculations will explore the role of nitrosyl bending in $[Cp^*Ru(NO)(mnt)]^{-\cdot}$.

### 2.5. Conclusions

The new cyclopentadienyl complex Cp*Ru(NO)(mnt) has been prepared and characterized by X-ray diffraction analysis and IR and NMR spectroscopies. Cp*Ru(NO)(mnt) exhibits both reversible one-electron oxidation and reduction behavior when examined by cyclic and rotating disk electrode voltametries in MeCN solvent; however, the $0/-1$ redox couple has been found to be unstable on the bulk electrolysis time scale. The nature of the HOMO and LUMO in Cp*Ru(NO)(mnt) has been established by extended Hückel molecular orbital calculations.

## 3. Experimental section

Disodium maleonitriledithiolate ($Na_2$mnt) [26] and Cp*Ru(NO)$Cl_2$ [48] were prepared according to published literature procedures. Methanol was degassed with argon immediately before each reaction. $CH_2Cl_2$ and MeCN were distilled from $CaH_2$ while THF was distilled from sodium/benzophenone. All solvents were distilled under argon using inert-atmosphere techniques and stored in Schlenk vessels equipped with Teflon stopcocks [49]. The tetra-*n*-butylammonium perchlorate used in the electrochemical studies was purchased from Johnson Matthey Electronics and recrystallized from ethyl acetate/petroleum ether. The C and H analysis was performed by Atlantic Microlab, Atlanta, GA.

Room temperature infrared spectra were recorded on a Nicolet 20 SXB FT-IR spectrometer in 0.1 mm NaCl cells. The low-temperature IR spectra were recorded on the same spectrometer using a Specac Model P/N 21.000 variable-temperature cell equipped with inner and outer $CaF_2$ windows. Dry ice/acetone was the coolant, and the cell temperature was determined with a copper-constantan thermocouple. The $^1H$ and $^{13}C$ NMR spectra were recorded on a Varian 200 VXR spectrometer at 200 and 50 MHz respectively.

### 3.1. Synthesis of Cp*Ru(NO)(mnt)

To 0.40 g (1.2 mmol) of Cp*Ru(NO)$Cl_2$ in 40 ml of MeOH was added 0.30 g (1.6 mmol) of disodium maleonitriledithiolate. The reaction was stirred overnight at room temperature, upon which time IR analysis revealed complete conversion to Cp*Ru(NO)(mnt). After the MeOH was removed, the crude product was taken up in $CH_2Cl_2$ and then chromatographed over silica gel using $CH_2Cl_2$ as the eluant. Recrystallization of Cp*Ru(NO)(mnt) from a $CH_2Cl_2$ solution containing Cp*Ru(NO)(mnt) that had been layered with heptane afforded both the analytical sample and single crystals suitable for X-ray diffraction analysis. Yield: 0.41 g (85%). IR ($CH_2Cl_2$): 2213 (m, CN), 2206 (m, CN), 1767 (s, NO) $cm^{-1}$. $^1H$ NMR ($CDCl_3$): $\delta$ 1.86 (Cp*). $^{13}C$ NMR ($CDCl_3$): $\delta$ 9.6 (Me), 111.5 (Cp* ring), 115.7 (CN), 125.8 (mnt C=C). Anal. Found C, 41.48; H, 3.75. $C_{14}H_{15}N_3ORuS_2$ calcd: C, 41.37; H, 3.72.

### 3.2. X-ray Crystallography

A black crystal of Cp*Ru(NO)(mnt) suitable for X-ray diffraction analysis, which was obtained after multiple crystallization attempts, of dimensions $0.18 \times 0.15 \times 0.44$ $mm^3$ was sealed inside a Lindemann capillary tube and mounted on the goniometer of an Enraf-Nonius CAD-4 diffraction. The radiation used was Mo K$\alpha$ monochromatized by a crystal of graphite. Cell constants were obtained from a least-squares refinement of 25 with $2\theta > 32°$. Intensity data in the range $2.0° \leq 2\theta \leq 40°$, which were collected at room temperature using the $\omega$ scan technique in the variable-speed mode, were corrected for Lorentz, polarization, and absorption (DIFABS). Three reflections (358, 080, 0014) were measured after every 3600 seconds of exposure time in order to monitor crystal decay, which was less than 2%. The structure was solved by using standard Patterson techniques, which revealed the position of the ruthenium atom. All remaining non-hydrogen atoms were located with difference Fourier maps and full-matrix least-squares refinement. With the exception of the carbon atoms, all non-hydrogen atoms were refined anisotropically. Refinement converged at $R = 0.043$ and $R_w = 0.049$ for 777 unique reflections with $F > 6\sigma(F)$.

### 3.3. Electrochemical measurements

Cyclic and rotating disk electrode voltammograms were obtained with a PAR Model 273 potentiostat/galvanostat using positive feedback circuitry to compensate for IR drop. The CV cell used was of airtight design and based on a three-electrode configuration, permitting all cyclic voltammograms to be recorded free from oxygen and moisture. The CV experiments utilized platinum disk (area = 0.0079 $cm^2$) working and auxiliary electrodes. The RDE voltammogram was recorded in a Vacuum Atmospheres Dribox at ambient temperature using a PAR Model 616 RDE unit. The working electrode consisted of a commercially available platinum disk electrode (area = 0.126 $cm^2$). Both the CV and RDE experiments employed a silver wire quasi-reference electrode, and all potential data are referenced to the formal potential of the $Cp_2Fe/Cp_2Fe^+$ redox couple run under identical conditions, taken to have an $E_{1/2} = 0.307$ V [35].

The bulk electrolysis experiments were conducted in the constant-potential mode in an air-tight cell with 0.25 M TBAP and the specified solvent. After the electrolysis was completed, the solution was examined by IR spectroscopy.

### 3.4. Molecular orbital calculations

The extended Hückel calculations conducted in this study were done with the original program developed by Hoffmann, [50], as modified by Mealli and Proserpio [44]. The atomic parameters used in this study were taken from the CACAO drawing program with all bond distances and angles used being taken directly from the X-ray crystallographic coordinates.

## Supplementary material available

Listing of observed and calculated structure factor amplitudes, tables of anisotropic thermal parameters, and idealized hydrogen parameters. Ordering information can be supplied by the authors upon request.

## Acknowledgments

We are especially grateful to Professor Carlo Mealli for providing us with a copy of his CACAO graphics program and to one of the reviewers for comments regarding the role of nitrosyl bending during reduction. We thank the Robert A. Welch Foundation (B-1202-SGB and B-1039-MGR) and the UNT faculty research program for continued financial support.

## References and notes

[1] G.N. Schrauzer, *Acc. Chem. Res.*, *2* (1969) 72.
[2] T.R. Miller and I.G. Dance, *J. Am. Chem. Soc.*, *95* (1973) 6970.
[3] I. Fischer-Hjalmars and A. Henrikson Enflo, *Adv. Quantum Chem.*, *16* (1982) 1.
[4] S.P. Best, S.A. Ciniawsky, R.J.H. Clark and R.C.S. McQueen, *J. Chem. Soc., Dalton Trans.*, (1993) 2267.
[5] D.G. VanDerveer and R. Eisenberg, *J. Am. Chem. Soc.*, *96* (1974) 4994.
[6] C.-H. Cheng and R. Eisenberg, *Inorg. Chem.*, *18* (1979) 1418.
[7] C.-H. Cheng and R. Eisenberg, *Inorg. Chem.*, *18* (1979) 2438.
[8] M.R. Churchill and J.P. Fennessey, *Inorg. Chem.*, *6* (1968) 1123.
[9] S.D. Henderson, T.A. Stephenson and E.J. Wharton, *J. Organomet. Chem.*, *179* (1979) 43.
[10] M. Sakurada, M. Kajitani, H. Hatano, Y. Matsudaira, T. Suetsugu, S. Ono, T. Akiyama and A. Sugimori, *Organometallics*, *11* (1992) 2337.
[11] J. Locke and J.A. McCleverty, *Inorg. Chem. 7* (1966) 1157.
[12] P. Thomas, M. Lippmann, D. Rehorek and H. Hennig, *Z. Chem.*, *20* (1980) 155.
[13] P. Thomas, D. Rehorek, V.I. Nefedov and E.K. Žumadilov, *Z. Anorg. Allg. Chem.*, *448* (1979) 167.
[14] J. Stach, R. Kirmse, W. Dietzsch and P. Thomas, *Z. Anorg. Allg. Chem.*, *480* (1981) 60.
[15] J.A. McCleverty, N.M. Atherton, J. Locke, E.J. Wharton and C.J. Winscom, *J. Am. Chem. Soc.*, *89* (1967) 6082.
[16] J.A. Zuleta, M.S. Burberry and R. Eisenberg, *Coord. Chem. Rev.*, *97* (1990) 47.
[17] J.M. Bevilacqua, J.A. Zuleta and R. Eisenberg, *Inorg. Chem.*, *32* (1993) 3689.
[18] J.A. Zuleta, J.M. Bevilacqua, D.M. Proserpio, P.D. Harvey and R. Eisenberg, *Inorg. Chem.*, *31* (1992) 2396.
[19] C.E. Johnson, R. Eisenberg, T.R. Evans and M.S. Burberry, *J. Am. Chem. Soc. 105* (1983) 1795.
[20] P. Bradley, C.E. Johnson and R. Eisenberg, *J. Chem. Soc., Chem. Commun.*, (1988) 255.
[21] E.G. Megehee, C.E. Johnson and R. Eisenberg, *Inorg. Chem.*, *28* (1989) 2423.
[22] A. Vogler and H. Kunkely, *J. Chem. Soc., Chem. Commun.*, (1986) 1616.
[23] V. Gama, R.T. Henriques, G. Bonfait, L.C. Pereira, J.C. Waerenborgh, I.C. Santos, M.T. Duarte, J.M.P. Cabral and M. Almeida, *Inorg. Chem.*, *31* (1992) 2598.
[24] V. Gama, R.T. Henriques, M. Almeida, L. Veiros, M.J. Calhorda, A. Meetsma and J.L. de Boer, *Inorg. Chem.*, *32* (1993) 3705.
[25] M.A. Greaney, C.L. Coyle, M.A. Harmer, A. Jordan and E.I. Stiefel, *Inorg. Chem.*, *28* (1989) 912.
[26] A. Davison and R.H. Holm, *Inorg. Chem.*, *10* (1967) 8.
[27] D.M.P. Mingos and D.J. Sherman, *Adv. Inorg. Chem.*, *34* (1989) 292.
[28] D.G.I. Felton and S.F.D. Orr, *J. Chem. Soc.*, (1955) 2170.
[29] D. Dolphin and A. Wick, *Tabulation of Infrared Spectral Data*, Wiley-Interscience, New York, 1977.
[30] G.C. Levy and G.L. Nelson, *Carbon-13 Nuclear Magnetic Resonance for Organic Chemists*, Wiley-Interscience, New York, 1972.
[31] I. Bernal, A. Clearfield, and J.S. Ricci, Jr., *J. Cryst. Mol. Sruct.*, *4* (1974) 43.
[32] C.G. Pierpont, A. Pucci and R. Eisenberg, *J. Am. Chem. Soc.*, *93* (1971) 3050.
[33] R. Eisenberg and C.D. Meyer, *Acc. Chem. Res.*, *8* (1975) 26.
[34] For examples of linear nitrosyl complexes with a distinctly non-linear M-nitrosyl bond angle, see: (a) J.A. Kaduk and J.A. Ibers, *Isr. J. Chem.*, *15* (1977) 143; (b) J.H. Enemark, *Inorg. Chem.*, *10* (1971) 1952; (c) C.P. Brock, J.P. Collman, G. Dolcetti, P.H. Farnham, J.A. Ibers, J.E. Lester and C.A. Reed, *Inorg. Chem.*, *12* (1973) 1304.
[35] A.J. Bard and L.F. Faulkner, *Electrochemical Methods*, Wiley, New York, 1980.
[36] J. Tomeš, *Coll. Czech. Chem. Commun.*, *9* (1937) 150.
[37] V.G. Levich, *Physicochemical Hydrodynamics*, Prentice Hall: Englewood Cliffs, NJ, 1962.
[38] (a) C.M.A. Brett and A.M.O. Brett, *Electrochemistry Principles, Methods and Applications*, Oxford University Press, New York, 1993; (b) where $R$ = gas constant; $T$ = absolute temperature; $r$ = molecular radius, which was obtained from the observed molecular volume of the crystal structure; $N$ = Avogadro's number; and $\eta$ = solvent viscosity.
[39] W.E. Geiger, P.H. Rieger, B. Tulyathan and M.D. Rausch, *J. Am. Chem. Soc.*, *106* (1984) 7000.
[40] For a review on the consequences of electrochemically induced structural changes, see W.E. Geiger, *Prog. Inorg. Chem.*, *33* (1985) 275.
[41] For related IR shifts in carbonyl and isonitrile ligands, see: (a) W.E. Geiger, N. Van Order, Jr., D.T. Pierce, T.E. Bitterwolf, A.L. Rheingold and N.D. Chasteen, *Organometallics*, *10* (1991) 2403; (b) J.P. Bullock and K.R. Mann, *Inorg. Chem.*, *28* (1989) 4006; (c) B.J. Brisdon, S.K. Enger, M.J. Weaver and R.A. Walton, *Inorg. Chem.*, *26* (1987) 3340; (d) Y. Zhang, D.K. Gosser, P.H. Rieger and D.A. Sweigart, *J. Am. Chem. Soc.*, *113* (1991) 4062; (e) J.P. Bullock, M.C. Palazotto and K.R. Mann, *Inorg. Chem.*, *30* (1991) 1284.
[42] T.A. Albright, J.K. Burdett and M.H. Whangbo, *Orbital Interactions in Chemistry*, Wiley-Interscience, New York, 1985.
[43] O. Hammerich and V.D. Parker in H. Lund and M.M. Baizer (eds.), *Organic Electrochemistry: An Introduction and Guide*, Dekker, New York, 1991, Chapter 3.
[44] C. Mealli and D.M. Proserpio, *J. Chem. Ed.*, *67* (1990) 399.
[45] (a) M.T. Ashby and J.H. Enemark, *J. Am. Chem. Soc. 108* (1986) 730; (b) A.D. Hunter, P. Legzdins, F.W.B. Einstein, A.C. Willis, B.E. Bursten and M.G. Gatter, *J. Am. Chem. Soc. 108* (1986) 3843.
[46] Unpublished results.
[47] For reports of electron accession at the nitrosyl ligand, see: (a) P. Legzdins, B. Wassink, F.W.B. Einstein and R.H. Jones, *Organometallics*, 7 (1988) 477; (b) D. Ballivet-Tkatchenko, B.

Nickel, A. Rassat and J. Vincent-Vaucquelin, *Inorg. Chem.*, *25* (1986) 3497; (c) P. Legzdins and B. Wassink, *Organometallics*, *7* (1988) 482.

[48] J.L. Hubbard, A. Morneau, R.M. Burns and C.R. Zoch, *J. Am. Chem. Soc. 113* (1991) 9176.

[49] D.F. Shriver, *The Manipulation of Air-Sensitive Compounds*, McGraw Hill, New York, 1969.

[50] (a) R. Hoffmann and W.N. Lipscomb, *J. Phys. Chem.*, *36* (1962) 2179; 3489; (b) R. Hoffmann, *J. Phys. Chem.*, *39* (1963) 1397.